PRE-PRINT ARTICLE

COPYRIGHT BY COMPOSITES THEORY AND PRACTICE JOURNAL

ISSN: 2299-128X

# Numerical analysis of the strength and stiffness of TRIGGO light electric vehicle body

Łukasz Stachowicz[1], Anna Boczkowska[2*], Rafał Budweil[1]

[1] TRIGGO S.A., Kolejowa 53, 05-092 Łomianki, Poland

[2]Warsaw University of Technology, Faculty of Materials Science and Engineering, Wołoska 141, 02-507 Warsaw, Poland

*Corresponding author: anna.boczkowska@pw.edu.pl

https://doi.org/10.62753/ctp.2025.01.1.1

**Abstract**

TRIGGO is one of the first vehicles to effectively combine the manoeuvrability and parking advantages of two-wheelers with the safety and comfort features comparable to those of small passenger cars. It is intended for use in a short-term rental network and should be characterised by low energy consumption. To this end, it is reasonable to optimise the vehicle's design towards minimising weight. The use of composites in the TRIGGO body structure enabled a reduction in the ready-to-drive vehicle weight and optimal utilisation of the available space. This choice makes it possible to keep the body weight low while ensuring appropriate mechanical properties. The subject of this paper is numerical analyses of the strength and stiffness of the TRIGGO light vehicle body made of glass-epoxy composites. The scope of the work includes the construction of a computational model of the TRIGGO vehicle body made by the RTM method with a double skin and foam core, in addition to calculations of the stiffness and strength of the structure during body load tests. For this purpose, an FEM computational model was built based on the 3D body model. The body of the RTM version of the TRIGGO vehicle consists of 27 separate components, which are connected to each other by rigid bonded contacts. The composite structures with foam cores were modelled as single-layer shell elements including all the layers of the composite, and a foam spacer. Three design cases were developed: P1.1 – vertical-transverse body loading, P1.2 – vertical-longitudinal body loading, P1.3 – vertical-longitudinal body loading with a horizontal force component. The calculation cases were determined based on "Regulation (EU) No 168/2013 of the European Parliament and of the Council with regard to requirements for the functional safety of vehicles for the approval of two- or three-wheel vehicles and quadricycles", in particular Annex XI of this document. The calculations prove that the glass-epoxy body of the TRIGGO light vehicle meets the requirements for strength and stiffness.

**Keywords**: TRIGGO electric car, automotive, FEM, GFRP, RTM, polymer matrix composites.

## Introduction

The problem of modern cities is pollution and traffic jams generated by the constantly increasing number of cars. A greater number of cars in city centres, combined with a constant (or even decreasing) number of parking spaces, has made it necessary for local authorities to change their approach to the organisation of traffic. The use of public transport, taxis or short-term vehicle rental (carsharing) is strongly promoted. At the same time, the creation of clean transport zones limits the possibility of entering city centres for older, less environmentally friendly vehicles.

PRE-PRINT ARTICLE

COPYRIGHT BY COMPOSITES THEORY AND PRACTICE JOURNAL

ISSN: 2299-128X

Polish Society of Composite Materials

The TRIGGO project is an attempt to address the above problems. TRIGGO is one of the first vehicles to effectively combine the manoeuvrability and parking advantages of two-wheelers with the safety and comfort features comparable to those of small passenger cars. Its capabilities are ensured by the patented design of the suspension with variable geometry.

The regulations for light vehicles in the L7e category, which include the TRIGGO vehicle, limit the weight of a ready-to-drive vehicle (excluding batteries) to 450 kg for the passenger subcategory and 600 kg for the cargo subcategory (Regulation (EU) No 168/2013, Annex I [1]). These limitations influenced the decision to use composites as the main construction material for the TRIGGO body. This choice makes it possible to keep the body weight low while ensuring the appropriate mechanical properties (strength and rigidity) [2].

The use of composites in the structure also enabled optimal utilisation of the available space. The passenger seat and safety belt anchorages have been integrated into the rear wall of the vehicle body. To ensure the safety of the vehicle occupants, it was also assumed that the structure should meet the optional requirements for a roll-overprotective structure (ROPS) (Commission Delegated Regulation (EU) Regulation No 3/2014, Annex XI [3]).

In the initial phase of vehicle production, glass-epoxy composites (GFRP) were used to construct the semi-monocoque body. A.S.SET single-component powder epoxy resin was employed for selected body parts [4]. For further production, it was planned to modify the body structure from a semi-monocoque to a monocoque design with a foam core, suitable for production using resin transfer moulding (RTM) technology.

Based on these assumptions, numerical analyses of two structural versions (semi-monocoque and monocoque) of the vehicle body were conducted. These analyses included calculations of the strength and stiffness during tests of the protective structure (ROPS) and calculations of the safety belt anchorages for the integrated passenger seat and driver's seat anchorages based on knowledge presented in [5-7].

The TRIGGO electric car, intended for use in a short-term rental network, should be characterised by low energy consumption. To this end, it is reasonable to optimise the vehicle's design towards minimising weight while maintaining active and passive safety features as well as utility values [8, 9]. The experience gained to date allows us to assume that the use of a similar design route will make it possible to significantly reduce the weight of the vehicle while maintaining its functional characteristics. To this end, it seems appropriate to carry out an analysis of the structural materials and production technologies available on the market to develop an optimum solution, which will meet the criteria of low weight, high strength and stiffness, ease of manufacturing the finished products, costs and environmental impact. This analysis should answer the question of whether the use of polymer composites would be justified in this case, or whether other alternative solutions should be favoured (e.g. light metal alloys, a combination of polymer composites and metal, the use of 3D printing or other solutions). Once the technology has been chosen, it is necessary to carry out in-depth optimisation of the design towards the appropriate use of composite materials by means of finite element method (FEM) analysis [10]. Due to the small size of the TRIGGO vehicle, there is no room for typical crumple zones, which need to be replaced with innovative elements capable of absorbing energy without an excessive increase in the vehicle's own weight [11].

PRE-PRINT ARTICLE

COPYRIGHT BY COMPOSITES THEORY AND PRACTICE JOURNAL

ISSN: 2299-128X

Polish Society of Composite Materials

The subject of this paper is numerical analyses of the strength and stiffness of the TRIGGO light vehicle body made of glass-epoxy composites. The scope of work includes the construction of a computational model of the TRIGGO vehicle body made by the RTM method with a double skin and foam core, in addition to calculations of the stiffness and strength of the structure during body load tests.

## Materials

The numerical calculations included 3 types of material:

1. Glass-epoxy laminate – a composite with layers of fabric arranged alternately every 45° or 60° to produce an isotropic structure, with combined thicknesses of 3 to 10 mm.

2. PVC foam – a foam core filling the spaces between the two layers of composite. It is present in the following components: the floor, left wall, right wall, back wall and in the two top connectors.

3. 2 mm thick S355 steel sections. Designed to be used in following components: rails for securing the driver's seat and a frame in the front section for securing components, the dashboard.

The material data for the calculation of the glass-epoxy laminate was obtained from previously conducted static tensile tests. Based on these, the properties of a single layer of glass-epoxy composite were developed, as shown in Table 1.

The designed laminate body consists of 3 layers of glass fabric of varying thicknesses with 0/90° fibre orientation in an epoxy matrix. A plot of Young's and Kirchhoff's modules for a single layer of the composite as a function of fibre direction is shown in Figure 1. Each fabric layer in the laminate is arranged at a 60° angle to its neighbour, resulting in a material with an approximate isotropic stiffness, as shown in Figure 2.

**Table 1. Material data of single layer of glass-epoxy composite used for TRIGGO body.**

| **Parameter** | | **Value** |
|---|---|---|
| Density $\rho$ [kg/m$^3$] | | 1900 |
| Young's modulus [MPa] | $E_{11}$ | 13900 |
| | $E_{22}$ | 4100 |
| Kirchhoff modulus $G_{12}$ [MPa] | | 1470 |
| Poisson's ratio $\nu_{12}$ | | 0.13 |

PRE-PRINT ARTICLE

COPYRIGHT BY COMPOSITES THEORY AND PRACTICE JOURNAL

ISSN: 2299-128X


**Figure 1. Young's and Kirchhoff's modules as a function of fibre direction for single layer of glass fabric.**

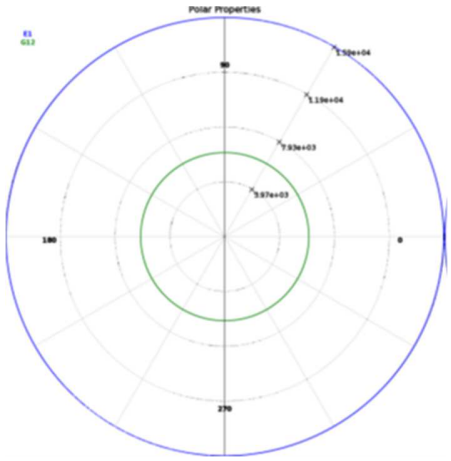


**Figure 2. Young's and Kirchhoff's modules as a function of fibre direction for laminate with 3 fabric layers.**

To model the poly(vinyl chloride) foam (PVC), which forms the core of the composite parts described earlier, an elastic material model with the properties specified in Table 2 was adopted.

**Table 2. Material data for PVC foam.**

| Parameter | Value |
|---|---|
| Density ρ [kg/m$^3$] | 115 |
| Young's modulus E [MPa] | 1000 |
| Poisson's ratio ν | 0.3 |

For the steel components made of S355 steel, a bi-linear material model was used with the parameters given in Table 3.

PRE-PRINT ARTICLE

COPYRIGHT BY COMPOSITES THEORY AND PRACTICE JOURNAL

ISSN: 2299-128X

**Table 3. Material data for S355 steel.**

| Parameter | Value |
|---|---|
| Density ρ [kg/m$^3$] | 7850 |
| Young's modulus E [MPa] | 200000 |
| Poisson's ratio ν | 0.3 |
| Yield stress Re [MPa] | 355 |
| Tangent modulus (consolidation) ET [MPa] | 860 |

## Computational model

ANSYS™ software was used for the FEM simulation studies. The FEM computational model shown in Figure 4 was built based on the 3D body model (Figure 1). The body of the RTM version of the TRIGGO vehicle consists of 27 separate components, which were connected to each other by rigid bonded contacts. The FE computational model was built using 2D shell elements (201,351 elements), and 3D solid elements (the foam core). The total number of elements in the model is 303,161, including 201,351 shell elements and 101,810 solid elements.

Composite structures with foam cores can be modelled as single-layer shell elements including all the layers of the composite, and a foam spacer [11]. Due to the complex geometry of this model and the varying thickness of the foam cores, it was decided to model the foam cores as solid elements and bonded to the outer layers of the surrounding composite using “Bonded contact”.

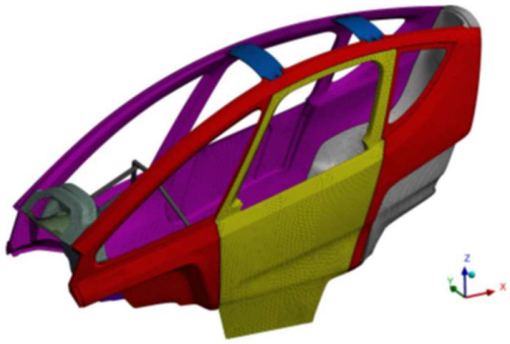

**Figure 3. FEM computational model of TRIGGO body made with RTM technology.**

The boundary conditions in the model were adopted to represent as faithfully as possible the actual fastening of the body to the vehicle frame. It was assumed that the body would be fastened to the frame by means of eight springs distributed as shown in Figure 4. The stiffnesses of these springs are given in Table 4. The fastening of the springs to the floor is carried out by means of rigid connectors connecting the upper and lower layers of the floor. The nodes to which the rigid connectors are applied are located at the radius of r=44mm from the springs (reinforcement area at the fastening points).

Rigid connectors between the plating layers were also used at the fastening points of the rear seat belt and at the fastening points of the front seat guides to the floor. The nodes to which the rigid connectors are applied are located at the radius of r=15.5 mm from these points.

PRE-PRINT ARTICLE
COPYRIGHT BY COMPOSITES THEORY AND PRACTICE JOURNAL
ISSN: 2299-128X

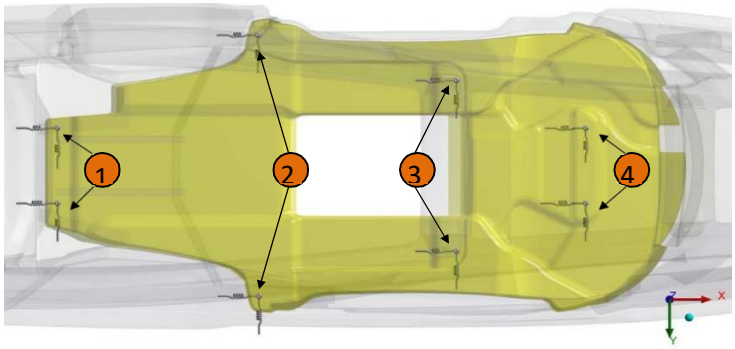


**Figure 4. TRIGGO composite body with body-to-floor fastening points.**

**Table 4. Spring stiffnesses at body fastening points.**

| Parameter | Fastening point number | | | |
|---|---|---|---|---|
| | 1 | 2 | 3 | 4 |
| kx [N/mm] | 120000 | 5000 | 12000 | 337000 |
| ky [N/mm] | 42500 | 100000 | 370000 | 15000 |
| kz [N/mm] | 10000 | 4000 | 13000 | 000 |

The design cases are defined based on [3] and, in particular Annex XI of that document. Annex XI describes the requirements for vehicles of category L7e-B2, which must be fitted with a roll-over protection structure (ROPS), as well as designed and constructed to meet the essential purpose of this Annex. This condition is deemed to be fulfilled if the provisions of paragraphs 2 to 4.9 are met, the protective structure does not enter the zone of clearance, and no part of the zone of clearance extends beyond the limits of the protective structure during the three tests.

Based on Annex XI of the Regulation [3], 3 design cases were developed:
P1.1 – vertical-transverse body loading.
P1.2 – vertical-longitudinal body loading.
P1.3 – vertical-longitudinal body loading with a horizontal force component.
The boundary conditions for all the design cases were the same as described above.

## Results

Vertical-transverse body loading (P1.1) consists of crushing the structure protecting the vehicle (roof) in the vertical direction, by a 150 mm wide rigid beam positioned transverse to the vehicle axis. The point of application of the beam is 300 mm in front of the R point of the driver's seat. In accordance with Section 3.1.2.5 of Annex XI [3], the crushing beam is applied in such a way that the load is evenly distributed horizontally (Figure 5). The calculation model for case P1.1 is shown in Figure 6. The test was carried out until the reaction force on the beam corresponding to double the weight of the vehicle, equal to Fz=11000 N, was reached.

PRE-PRINT ARTICLE

COPYRIGHT BY COMPOSITES THEORY AND PRACTICE JOURNAL

ISSN: 2299-128X

Polish Society of Composite Materials

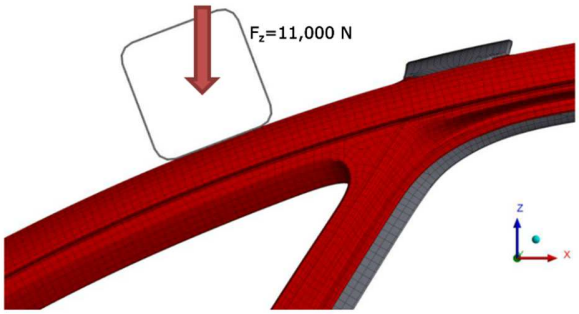


**Figure 5. Crushing beam placement for vertical-transverse loading – P1.1.**

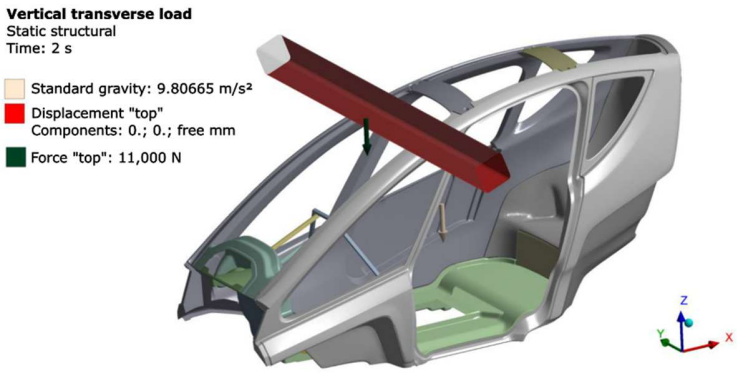


**Figure 6. Design model for vertical-transverse loading – P1.1.**

The simulation results in the form of displacement maps of the structure are shown in Figures 7-10. The maximum total displacements for the P1.1 load case occur at the contact points between the body and the crushing beam and are 12 mm (Figure 7). At the same time, maximum vertical displacements of 8.7 mm towards the underside of the vehicle occur at this location (Figure 8). The maximum longitudinal displacement is 8.5 mm towards the rear of the vehicle (Figure 9). The maximum transverse displacement is 4.5 mm and is shown in Figure 10.

PRE-PRINT ARTICLE

COPYRIGHT BY COMPOSITES THEORY AND PRACTICE JOURNAL

ISSN: 2299-128X

Polish Society of Composite Materials

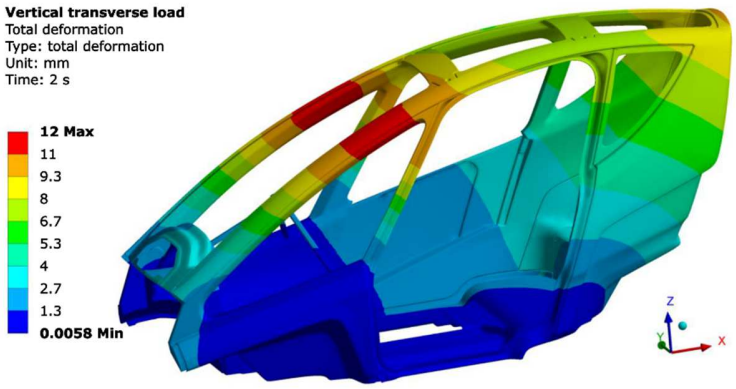


**Figure 7. Resultant displacements – case P1.1.**

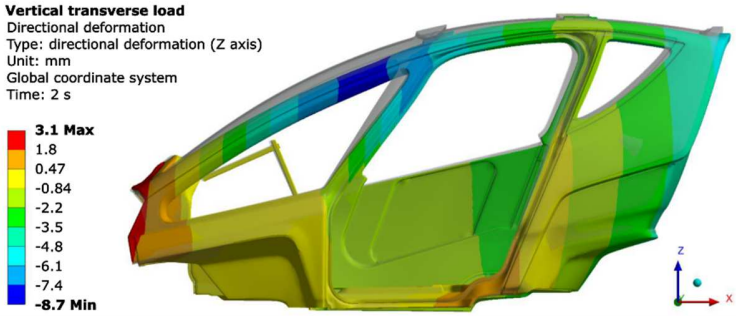


**Figure 8. Vertical displacements (Z axis) – case P1.1 (displacement scale x5).**

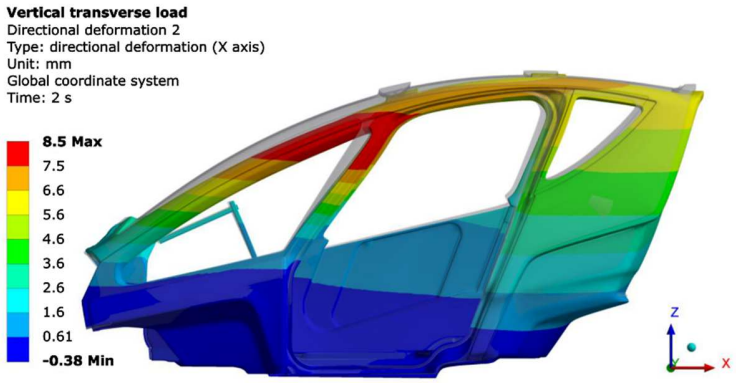


**Figure 9. Longitudinal displacements (X axis) – case P1.1 (displacement scale x5).**

PRE-PRINT ARTICLE

COPYRIGHT BY COMPOSITES THEORY AND PRACTICE JOURNAL

ISSN: 2299-128X

Polish Society of Composite Materials

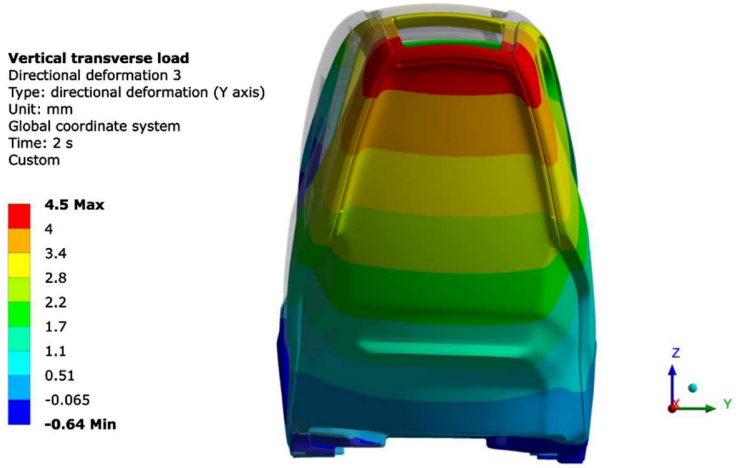


**Figure 10. Transverse displacements (Y axis) – case P1.1 (displacement scale x10).**

Maps of normal stresses in the principal fibre directions for the entire laminate cross-section (double-sided display for the outer top and inner bottom layers) are shown in Figures 11-13. The maximum tensile stress is 49 MPa, while the compressive stress is 76 MPa and they occur in the top cross-section of the right side of the vehicle near the 'B-pillar'.

Figures 14 and 15 present shear stress maps in the fibre plane. The maximum value of these stresses is 39 MPa and it occurs in the right 'B-pillar'. The normal and shear stresses in the laminate do not exceed the strength limits of the material. The reduced stresses in the steel frame reach a maximum value of 58 MPa and is within the elastic working range of the material (Figure 16).

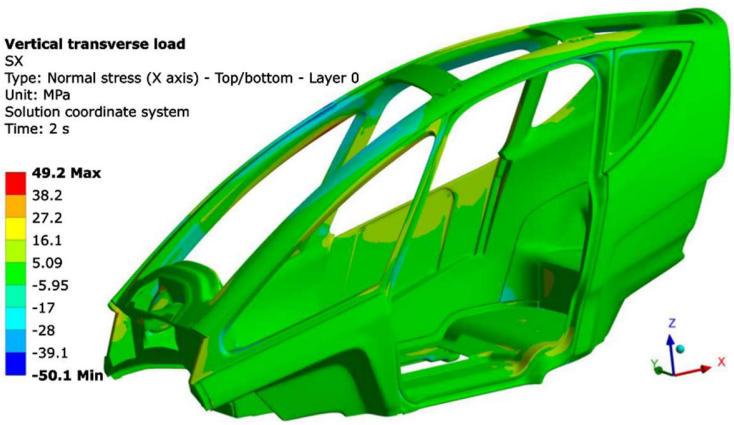


**Figure 11. Normal stresses in 0° fibre direction – case P1.1.**

PRE-PRINT ARTICLE

COPYRIGHT BY COMPOSITES THEORY AND PRACTICE JOURNAL

ISSN: 2299-128X

Polish Society of Composite Materials

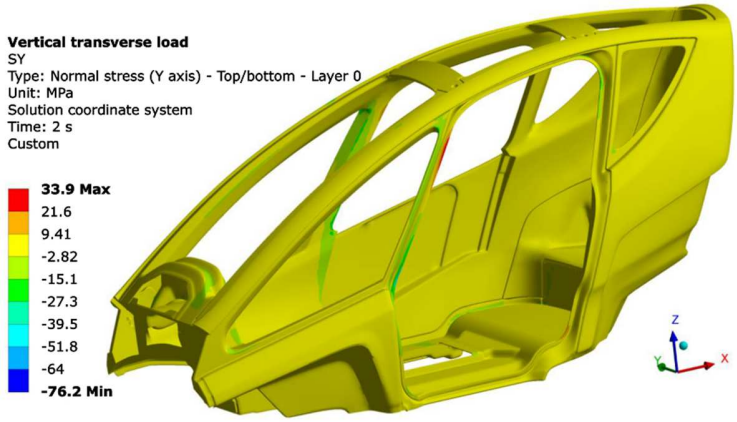


**Figure 12. Normal stresses in direction perpendicular to 0° fibre direction – case P1.1.**

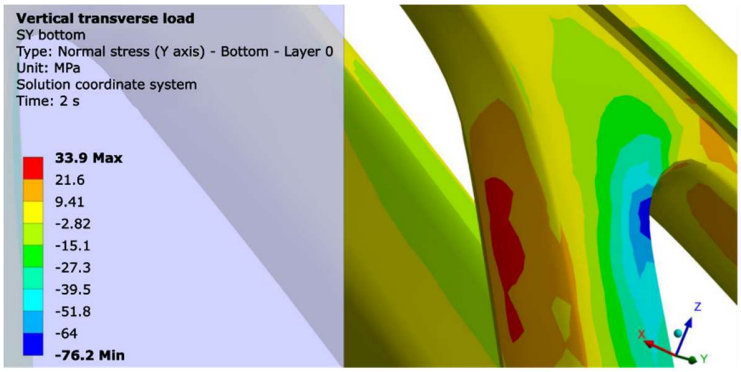


**Figure 13. Normal stresses in direction perpendicular to the 0° fibre – stress concentrations on right front pillar – case P1.1.**

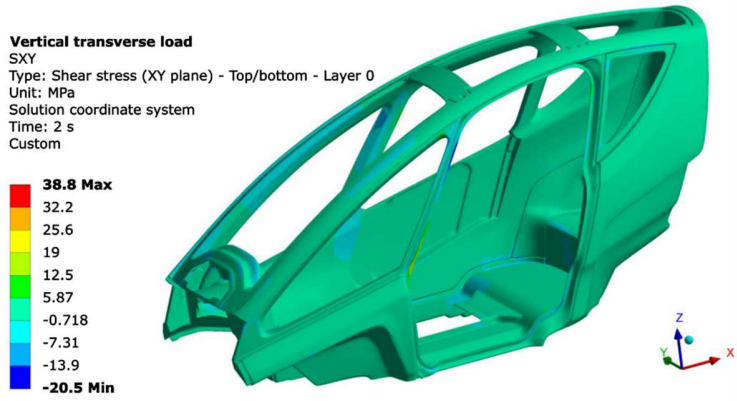


**Figure 14. Shear stresses in plane of main material axes – case P1.1.**

PRE-PRINT ARTICLE

COPYRIGHT BY COMPOSITES THEORY AND PRACTICE JOURNAL

ISSN: 2299-128X

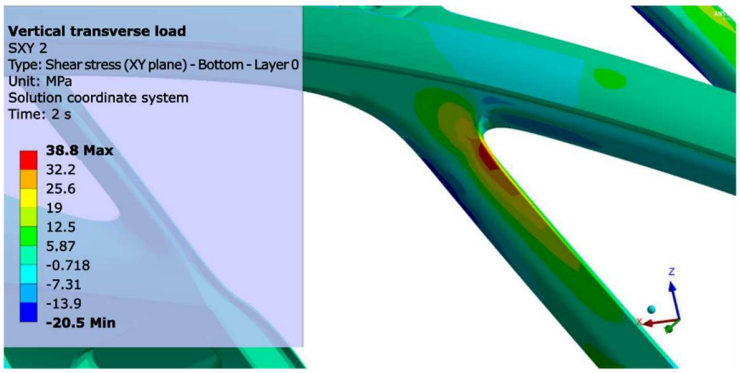


**Figure 15. Shear stresses in plane of main material axes – view of connection between right B-pillar and top crossbar – case P1.1.**

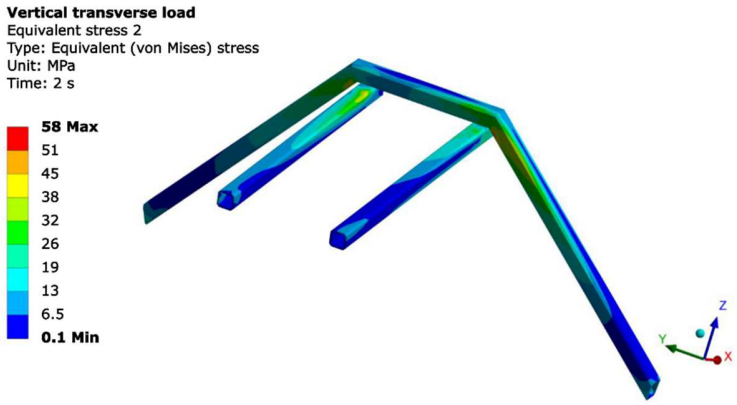


**Figure 16. Reduced stresses in steel front frame – case P1.1.**

Figure 17 shows the measured distances between the driver and passenger models and the surface of the deformed vehicle roof. The values of these distances in the undeformed state are 53.5 mm for the driver and 89.2 mm for the passenger. In the deformed state, these distances decrease to 47.6 mm for the driver and 85.1 mm for the passenger, representing a reduction in ground clearance of 5.9 mm and 4.1 mm, respectively.

PRE-PRINT ARTICLE
COPYRIGHT BY COMPOSITES THEORY AND PRACTICE JOURNAL
ISSN: 2299-128X
Polish Society of Composite Materials

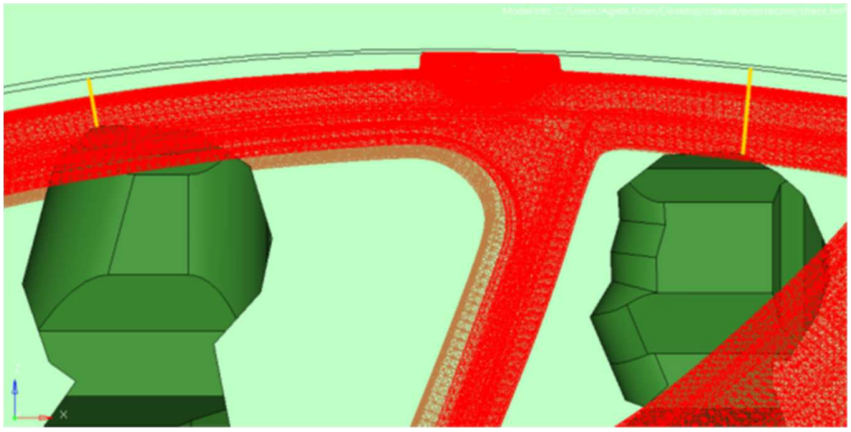

**Figure 17. Free space zone measurement (yellow line) – case P1.1.**

Figures 18-21 display the realisation of the subsequent loading cases, i.e. P1.2 – vertical-longitudinal body loading and P1.3 – vertical-longitudinal body loading with a horizontal force component, respectively. Loading P1.2 consists of crushing the structure protecting the vehicle (roof) in the vertical direction by means of a rigid beam 150 mm wide positioned longitudinally to the vehicle axis. The point of application of the beam is located at a distance equal to one-sixth of the overall width of the upper third of the structure. In accordance with Section 3.1.2.5 of Annex XI [3], the crushing beam is applied so that the load is evenly distributed horizontally (Figure 18). The calculations were carried out for the case where the crushing beam was located on the left side of the vehicle. This is because the body structure is 'weakened' at this location by the door opening, and is therefore the more unfavourable case. The calculation model for this case is shown in Figure 19. The test was carried out until the reaction force on the beam corresponding to double the weight of the vehicle, equal to Fz=11,000 N, was reached.

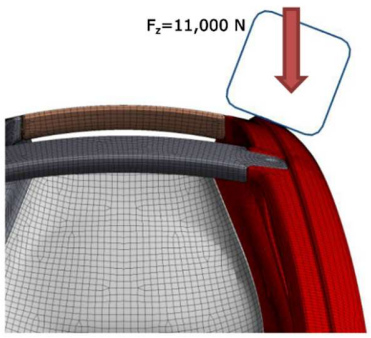


**Figure 18. Crushing beam position for vertical-longitudinal loading – P1.2.**

PRE-PRINT ARTICLE

COPYRIGHT BY COMPOSITES THEORY AND PRACTICE JOURNAL

ISSN: 2299-128X

Polish Society of Composite Materials

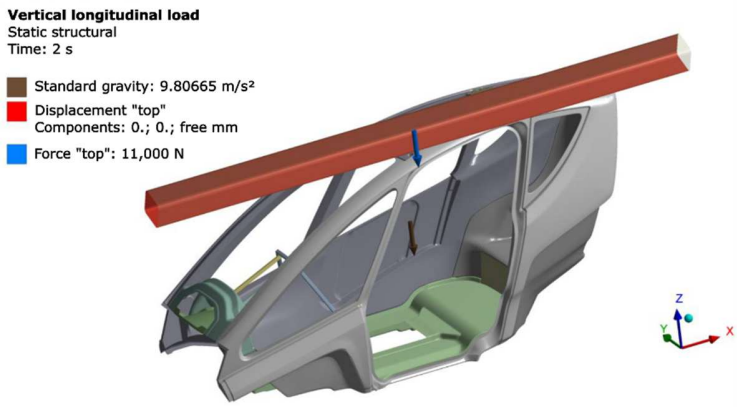


**Figure 19. Vertical-longitudinal loading design model – P1.2.**

Loading P1.3, on the other hand, consists in crushing the structure protecting the vehicle (roof) in the vertical direction with prior displacement of the structure in the horizontal direction. The crushing element consists of a 150 mm wide rigid beam positioned longitudinally to the vehicle axis. The point of application of the vertical crushing beam is at the same location as for loading P1.2, while the point of application of the horizontal crushing beam is at the edge of the vehicle roof. In accordance with Section 3.1.2.5 of Annex XI [3], the crushing beams are applied so that the load is uniformly distributed horizontally (Figure 20). The calculation model for this case is shown in Figure 21. The test was carried out in such a way that first a force of Fy=2,750 N (0.5 x vehicle weight) was applied to the horizontal crushing beam and then, after deformation of the structure, a force of Fz=5,500 N (0.5 x Fzmax, where Fzmax is the vertical force value from case P1.2) was applied to the vertical crushing beam.

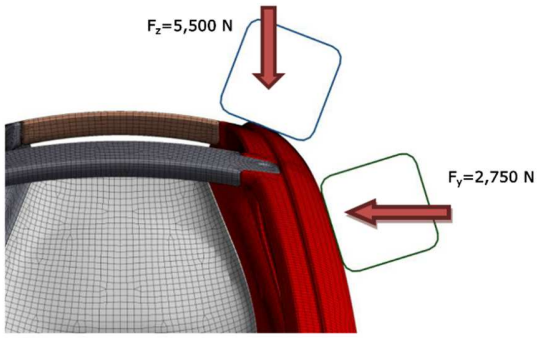


**Figure 20. Position of crushing beams for vertical-longitudinal loading with horizontal force component – P1.3.**

PRE-PRINT ARTICLE

COPYRIGHT BY COMPOSITES THEORY AND PRACTICE JOURNAL

ISSN: 2299-128X

Polish Society of Composite Materials

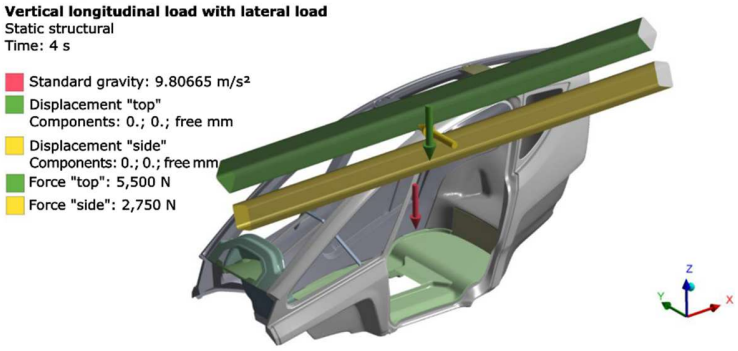


**Figure 21. Vertical-longitudinal loading with horizontal force component design model – P1.3.**

The FEA calculations for cases P1.2 and P1.3 were carried out in the same way as for case P1.1, considering the respective loading method. The maximum total displacement for the P1.2 load case occur at the contact points between the body and the crushing beam and is 15.5 mm. At the same time, there is a maximum vertical displacement of 12.8 mm towards the underside of the vehicle. The maximum longitudinal displacement is 6.9 mm towards the rear of the vehicle. Deformation can be observed in the C-pillar, which takes most of the load from the crushing beam. The maximum transverse displacement is 8.2 mm towards the right side of the vehicle (Figure 22).

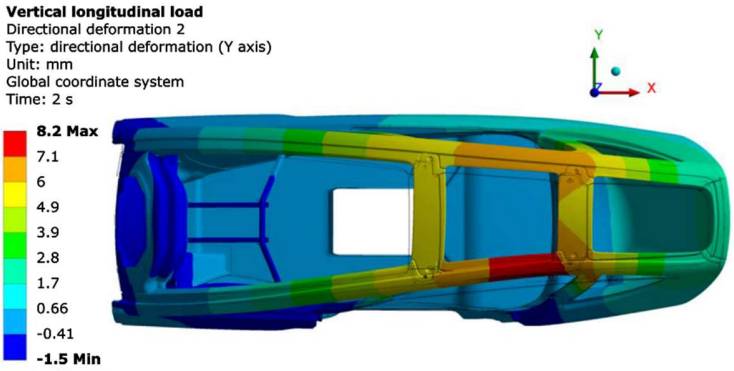


**Figure 22. Transverse displacements (Y axis) – case P1.2 (displacement scale x5).**

The determined maximum tensile stress for case P1.2 is 108 MPa, which occurs in the left upper bar at the junction with the C-pillar. The maximum compressive stress is 115 MPa and it occurs in the left C-pillar. The maximum shear stress is 52.1 MPa, occurring in the left C-pillar. The normal and shear stresses in the laminate do not exceed the strength limits of the material. The reduced stresses in the steel frame reach a maximum value of 53 MPa and are within the elastic working range of the material.

Analogous to case P1.2, the distances between the driver and passenger models and the surface of the deformed vehicle roof were also measured in this case. The values of these distances in the undeformed state are 53.5 mm for the driver and 89.2 mm for the passenger. In the deformed state, these distances decrease to 47.1 mm for the driver and 83.7 mm for the passenger, which means a reduction in ground clearance of 6.4 mm and 5.5 mm respectively.

PRE-PRINT ARTICLE

COPYRIGHT BY COMPOSITES THEORY AND PRACTICE JOURNAL

ISSN: 2299-128X

For case P1.3, the maximum total displacement occurs at the body-crushing beam interface and it is 14.5 mm. At the same time, there is a maximum vertical displacement of 7.2 mm towards the underside of the vehicle. The maximum longitudinal displacement is 3.3 mm towards the rear of the vehicle. The maximum transverse displacement is 14.5 mm, originating from the force induced by the side beam and directed towards the right side of the vehicle.

The maximum tensile stress for case P1.3 is 69.3 MPa, which occurs in the left upper crossbar at the junction with the C-pillar. The maximum compressive stress is 70.4 MPa, occurring in the left upper crossbar near the rear link. Figures 48 and 49 show the maps. The maximum shear stress in the fibre plane is 29.7 MPa and it occurs in the left C-pillar. The normal and shear stresses in the laminate do not exceed the material strength limits. The reduced stresses in the steel frame reach a maximum value of 47 MPa and are within the elastic working range of the material.

The distances between the driver and passenger models and the surface of the deformed vehicle roof were measured in the vertical and transverse directions. In the undeformed state, these distances in the vertical direction are 53.5 mm for the driver and 89.2 mm for the passenger. In the deformed state, the distances in the vertical direction decrease to 48.2 mm for the driver and 85.8 mm for the passenger, which means a reduction in ground clearance of 5.3 mm and 3.4 mm respectively. In the undeformed state, the minimum distances in the transverse direction are 89.6 mm for the driver and 61.5 mm for the passenger. In the deformed condition, the distances in the transverse direction reduce to 78.5 mm for the driver and 58.2 mm for the passenger, which means a reduction in ground clearance of 11.1 mm and 3.3 mm respectively.

Table 5 summarises all the obtained values and the locations of the maximum normal and reduced stresses for all the presented load cases.

**Table 5. Values and locations of maximum stresses for each design case.**

| Calculation cases | Maximum normal tensile stress, [MPa] | Maximum normal compressive stress, [MPa] | Maximum shear stress, [MPa] |
|---|---|---|---|
| P.1.1 | 49.2 | 76.2 | 39.0 |
| | Right upper bar | Right B-pillar | Right B-pillar |
| P.1.2 | 108.0 | 115.0 | 52.1 |
| | Left upper bar near C-pillar | Left C-pillar | Left C-pillar |
| P.1.3 | 69.3 | 70.4 | 29.7 |
| | Upper left transom near the rear link | Upper left transom near the rear link | Left C-pillar |

## Conclusions

The TRIGGO composite body designed to date has confirmed the validity of using composite materials to obtain a fully functional, safe and light product.

FEM calculations were performed for the body of the TRIGGO light vehicle in the RTM version according to the documentation and assumptions made. The calculation cases were determined based on "Regulation (EU) No 168/2013 of the European Parliament and of the Council with regard to requirements for the

PRE-PRINT ARTICLE

COPYRIGHT BY COMPOSITES THEORY AND PRACTICE JOURNAL

ISSN: 2299-128X

functional safety of vehicles for the approval of two- or three-wheel vehicles and quadricycles", in particular Annex XI of this document.

The performed calculations demonstrate that the body of the TRIGGO light vehicle meets the requirements for body strength (ROPS) when the vehicle rolls over.

In the next step, experimental tests will be performed on the real TRIGGO vehicle body (a semi-monocoque structure), including a load test on the roll-overprotective structure, as well as the safety belt and driver's seat anchorages [12]. The aim of the research will be to compare the results of the numerical analyses conducted during the TRIGGO project with the results obtained from experimental tests.

**Acknowledgements**

The work was carried out under the project POIR.01.02.00-00-0285/16 entitled. "Special body with increased durability for the variant of the "L" category vehicle with increased mobility "Triggo", intended for operation in automatic rental networks "carsharing", and the technology of serial production of its elements based on innovative epoxy resins A.S.SET.", funded by National Centre of Research and Development.

**References**

[1] Regulation (EU) No 168/2013 of the European Parliament and of the Council on the approval and market surveillance of two- or three-wheel vehicles and quadricycles

[2] A. Elmarakbi, Advanced composite materials for automotive applications. Structural integrity and crashworthiness, 2014

[3] Commission Delegated Regulation (EU) No 3/2014 supplementing Regulation (EU) No 168/2013 of the European Parliament and of the Council with regard to vehicle functional safety requirements for the approval of two- or three-wheel vehicles and quadricycles

[4] A. Boczkowska, Ł. Stachowicz, R. Budweil, Development of a method for producing composite parts of the TRIGGO electric car based on A.S.SET epoxy resin powder – feasibility study, Composites Theory and Practice 24: 4 (2024)https://doi.org/10.62753/ctp.2024.06.4.4

[5] WAT, Substantive report on research work. Experimental research on the strength of the TRIGGO vehicle body, 2021

[6] CIM-mes, Vehicle body strength testing. Part 1: performance of static-dynamic analyses of the rollover protective structure (ROPS) and seat belt anchorage points, 2019

[7] CIM-mes, Testing the strength of the body of the TRIGGO vehicle in RTM version, 2020.

[8] Y. Chen, G. Liu, Z. Zhang, *et al.* Integrated design technique for materials and structures of vehicle bodies under crash safety considerations. Structural and Multidisciplinary Optimization 56, 455-472 (2017), https://doi.org/10.1007/s00158-017-1674-8

[9] E. Mangino and E. Indino, The use of composite materials in vehicle design, Design and Structural Simulation of Composites in Transportation 2002 (Genoa).

ISSN: 2299-128X

[10] P. K. Mallick, Materials, Design, and Manufacturing for Lightweight Vehicles, 2021

[11] S. Borazjani, G. Belingardi, Development of an innovative design of a composite-sandwich based vehicle roof structure, Composites Structures 168, 522-534 (2017), https://doi.org/10.1016/j.compstruct.2017.02.015

[12] ISO 3471:2008, Earth-moving machinery - Roll-overprotective structures - Laboratory tests and performance requirements